Molecular Complex of Cholecystokinin-8 and N-Terminus of the Cholecystokinin A Receptor by NMR Spectroscopy‡

Maria Pellegrini§ and Dale F. Mierke*,§,||

Department of Molecular Pharmacology, Division of Biology & Medicine, and Department of Chemistry, Brown University, Providence, Rhode Island 02912

Received June 3, 1999; Revised Manuscript Received August 20, 1999

ABSTRACT: The bimolecular complex of the C-terminal octapeptide of cholecystokinin, CCK-8, with the N-terminus of the CCK_A-receptor, CCK_A-R(1−47), has been structurally characterized by high-resolution NMR and computational refinement. The conformation of CCK_A-R(1−47), within the lipid environment used for the spectroscopic studies, consists of a well-defined α-helix (residues 3−9) followed by a β-sheet stabilized by a disulfide linkage between C18 and C29, leading to the first transmembrane α-helix (TM1). Titration of CCK_A-R(1−47) with CCK-8 specifically affects the NMR signals of W39 of the receptor, in a saturable fashion. This association is specific for CCK-8; no association was observed upon titration of CCK_A-R(1−47) with other peptide hormones. The ligand/receptor complex was characterized by intermolecular NOEs between Tyr^{27} and Met^{28} of CCK-8 and W39 of CCK_A-R(1−47). These findings suggest that CCK-8 binds to CCK_A with the C-terminus within the seven-helical bundle and the N-terminus of the ligand, projecting out between TM1 and TM7, forming specific interactions with the N-terminus of the CCK_A receptor. This mode of ligand binding, consistent with published mutagenesis studies, requires variation of the interpretation of recent findings from photoaffinity cross-linking studies.

Cholecystokinin (CCK)[1] is a regulatory peptide hormone active through two distinct G-protein coupled receptors: the CCK_A (CCK_A-R) and CCK_B (CCK_B-R) receptors located predominantly in the gastrointestinal tract and in the central nervous system, respectively (*1*−*4*). CCK exists physiologically in multiple forms of varying length sharing the C-terminal sequence. The cholecystokinin octapeptide (CCK 26−33 or CCK-8) and larger forms display similar high affinity for the two receptors, while shorter, C-terminal CCK fragments are more selective for CCK_B-R, although with reduced affinity (*4*).

Attempts to characterize the molecular basis of CCK binding to CCK_A-R utilizing two different approaches (mutagenesis and photoaffinity cross-linking) have recently appeared in the literature (*5*−*13*). These data have lead to contrasting conclusions as to the binding mode of CCK to CCK_A-R; conclusions differing in most of the specifics including the residues of CCK involved in the ligand/receptor interaction and the orientation of the ligand in the binding pocket, as well as the structure of the bound agonist peptide. This discrepancy can be attributed to the fundamental differences of the methods utilized (*5*, *6*, *10*); both techniques require significant modifications of the system, either the receptor (mutagenesis studies) or the ligand (photoaffinity labeling).

A number of studies correlating mutations and/or receptor chimera of CCK_A-R and CCK_B-R with the binding and biological profiles of ligands have appeared (*5*−*9*, *14*). However, problems with alteration of receptor function via indirect mechanisms, producing local conformational effects or altering the processing or trafficking of the receptor have been noted (*15*). Additionally, it is seldom possible to correlate a specific mutation of the receptor with a corresponding interaction site on the peptide [although some exceptions have appeared (*6*, *12*)].

Photoaffinity labeling of the receptor via cross-linking to an appropriately modified ligand provides direct evidence of a contact point, or contact domain, between CCK and CCK_A-R (*10*, *11*). The drawback to this method is the requirement of ligand modification: the introduction of a photoactive moiety for cross-linking and a radio-label (often ^{125}I and/or Bolton−Hunter modification). The photolabile moieties [i.e., p-NO_2 substitution of phenylalanine or benzoylphenylalanine (Bpa) (*16*)] cannot be expected to interact with the receptor in the same manner as the naturally occurring residues they are replacing. These problems are particularly significant for a small ligand such as CCK-8, in which the iodination and photolabeling sites are necessarily close to each other and to the residue determinant for binding to the receptor. Photoactive centers may also suffer from varying reactivity toward target alkyl groups (*17*).

‡ The structure coordinates have been deposited in the Brookhaven Protein Data Bank (filename 1D6G).

* To whom correspondence should be addressed. Phone: (401) 863-2139. Fax: (401) 863-1595. E-mail: Dale_Mierke@Brown.edu.

§ Department of Molecular Pharmacology.

|| Department of Chemistry.

[1] Abbreviations: CCK, cholecystokinin; CCK_A-R, cholecystokinin type A receptor; CCK_B-R, cholecystokinin type B receptor; DG, distance geometry; DPC, dodecylphosphocholine; doxyl, 4,4-dimethyl-3-oxazolidinyloxy; DQF-COSY, double quantum filtered correlation spectroscopy; MD, molecular dynamics; NMR, nuclear magnetic resonance; NOE, nuclear Overhauser enhancement; NOESY, nuclear Overhauser enhancement spectroscopy; RMSD, root-mean-square deviation; ECL, extracellular loop; G-Protein, guanine nucleotide-binding regulatory protein; TM, transmembrane; TOCSY, total-correlation spectroscopy.

10.1021/bi991272l CCC: $18.00
Published on Web 10/21/1999

To address these issues, we have undertaken an experimental examination of the receptor/ligand complex. Here, we describe the spectroscopic characterization of the ligand, CCK-8, the receptor fragment, CCK_A-R(1−47), and the bimolecular complex of the two. The receptor fragment, CCK_A-R(1−47), was designed to encompass the entire extracellular N-terminal domain and a few residues of the first transmembrane helix (TM1) to assist in tethering the fragment to the membrane-mimetic environment used in the spectroscopic studies. Upon titration of the receptor with ligand, a definite, saturable shift of the ^{1}H NMR signals of W39 of the receptor[2] was observed. Intermolecular NOEs clearly show Tyr^{27} and Met^{28} of CCK-8 (utilizing the numbering of CCK-33) in close contact with W39 in the complex. With the structural features of the complex determined here, the mode of binding of this important peptide hormone to CCK_A can be addressed.

EXPERIMENTAL PROCEDURES

Peptide Synthesis. The receptor fragment CCK_A-R(1−47), consisting of the first 47 amino acids of the human CCK_A receptor, with free amino- and carboxy-termini, was synthesized by solid-phase methodology at the Protein Chemistry Facility of Tufts University (Boston, MA) using Fmoc chemistry and an Applied Biosystems peptide synthesizer. Analytical high-performance liquid chromatography and mass spectrometry established the purity and the structural integrity, respectively. The peptide CCK-8 (D^{26}YMGWMDF^{33}-NH_2) was purchased from Phoenix Pharmaceutics Inc. (Mountain View, CA; purity ≥ 95%).

NMR Methods. CCK_A-R(1−47) was examined in aqueous solution (ca. 1.6 mM, 9:1 $H_2O/^2H_2O$) or D_2O solution (99.8%, Cambridge Isotopes), pH 6.5, not corrected for isotope effect, in the presence of 171 mM dodecylphosphocholine-d_{38} (DPC, Cambridge Isotopes). The solution of CCK-8 contained 1.5 mM peptide (9:1 H_2O:^2H_2O, pH 6.5, not corrected) and 137 mM DPC-d_{38}. The experiments were recorded on a Varian Unity500 and a 750 MHz spectrometer (Massachusetts Institute of Technology, Boston, MA) for CCK_A-R(1−47) and on a Bruker Avance 600 MHz for CCK-8 at temperatures varying between 285 and 318 K. Data processing utilized Varian software (VNMR), Felix (Molecular Simulations Inc.), or NMRPipe (*18*). Chemical shifts were referenced to the signal of tetramethylsilane (0.0 ppm).

The amino acid spin systems were identified from DQF-COSY (*19*) and TOCSY (*20*, *21*) (mixing times of 15−75 ms) spectra. NOESY (*22*, *23*) experiments with mixing times of 100−350 ms were employed for the sequential assignment. Suppression of the solvent signal was achieved by continuous wave presaturation at low power during the relaxation delay (1.5−2 s) or WATERGATE (*24*, *25*). Some of the NOESY experiments utilized additional presaturation during the mixing time or, alternatively, coupled a "jump and return" observation pulse (*26*) with 0.4 s of presaturation. Forward linear prediction to 1024 points was applied to the incremented dimension; both dimensions were multiplied by Gaussian or shifted squared sine bell apodization functions, prior to Fourier transformation. Secondary shifts for Hα were calculated by subtracting the chemical shifts for unstructured peptides (*27*) from the experimentally measured chemical shifts and averaging the values over five residues (*28*).

The 1D experiments on the complex between CCK_A-R(1−47) and CCK-8 were carried out on a 0.8 mM solution of CCK_A-R(1−47) in D_2O (99.9% D_2O Cambridge Isotopes, pH 6.5, $T = 298$ K, 500 MHz) in DPC, to which successive aliquots of ca. 250 μg of solid CCK-8 were added up to a total of 2 mg of peptide ligand (0.37 to 3 mM of CCK-8). The concentration of the receptor fragment was doubled for the 2D TOCSY and NOESY, recorded as described for CCK_A-R(1−47), to achieve a better signal-to-noise ratio for the less sensitive experiments. A parallel titration was carried out on an identical solution of CCKA-R(1−47) in DPC by addition of two aliquots (0.8 mg) of the unrelated undecapeptide Lys-Kallidin (K-K-R-P-P-G-F-S-P-F-R). The titration was monitored via 1D spectra and 2D TOCSY and NOESY to investigate the specificity of the CCK-8/CCK_A-R(1−47) association.

Radical-Induced Relaxation. The 5-doxylstearic acid was solubilized in methanol-d_4 to a final concentration of 53.3 mM. Aliquots of this solution were added to the solution of peptide and DPC to obtain 0.35−1.4 mM concentrations of the spin-label. TOCSY experiments (mixing time 50 ms) were recorded under identical conditions before and after the addition of the doxylstearic acid. The intensities of cross-peaks involving both backbone (H^N-H^α) and side-chain protons ($H^\alpha-H^\beta$, $H^\gamma-H^\delta$) were compared.

Structure Calculation. For the structural characterization of CCK_A-R(1−47), NOESY spectra acquired at 298, 308, and 318 K with a mixing time of 150 ms were utilized to measure cross-peaks volumes. The volumes were converted to distances utilizing three classes according to the intensity: 1.8−3.0, 1.8−4.0, and 1.8−5.0 Å. The initial structure was built using InsightII (Molecular Simulations Inc). MD simulations were performed with GROMACS, version 1.6 (*29*). The structure was energy minimized (steepest descent) and soaked in a two-phase box of H_2O/decane, containing 6291 water and 300 decane molecules in a volume of 464.5 nm^3. This biphasic simulation cell was implemented to provide conditions consistent with the experimental system (water and DPC micelles) and acceptable computation times on standard workstations (*30*). A detailed description of the H_2O/decane interface has appeared (*31*). The charges of ionizable groups correspond to the pH of the NMR solution; no counterions were included. The system was energy minimized for 200 steps (steepest descent). During the following 10 ps of MD at 300 K (*32*) all protein heavy atoms were restrained to the original position with a force constant of 1000 kJ mol^{-1} nm^{-1}, to allow the solvent to equilibrate. Experimental distance restraints were then introduced with a force constant of 500 kJ mol^{-1} nm^{-1}. A weak restraining potential (10 kJ mol^{-1} nm^{-1}) was applied to the ϕ and ψ angles of residues 4−7 and 37−44. The following step consisted in two cycles of a robust simulated annealing protocol (each cycle 80 ps from 1000 to 300 K in 0.02 ps steps, applying the linear constraint solver LINCS on all bonds) (*33*). The restraints on dihedral angles were then removed and 250 ps of molecular dynamics at 300 K were carried out. A twin-range cutoff for nonbonded forces of 1.0 nm was used. Structures were sampled every 0.5 ps. The

[2] To simplify the description of the interaction in the ligand/receptor complex, the amino acids of the ligand will be denoted using the three-letter code, while the one letter code will be used for the residues of the receptor.

250 ps of MD simulation were completed in 18 h utilizing four processors on a SGI Origin 2000 (R10000, 195 MHz, 2 GB of RAM). The resulting trajectories were examined with analysis programs in the GROMACS package and home-written C programs.

The structural features of CCK-8 were determined utilizing cross-peaks volumes measured from NOESY spectra acquired at 298 and 308 K with mixing times of 100 and 150 ms. The volumes were converted to distances, with addition and subtraction of 10% to produce upper and lower bounds, respectively, using the resolved cross-peak between methylene protons of Asp^{26} as a reference (1.78 Å) (*27*, *34*). Pseudoatom corrections were applied to aromatic groups and methylene protons with coincident chemical shifts (*35*); the floating chirality approach (*36*) was utilized for resolved, nonstereospecifically-assigned methylene protons.

A home-written distance geometry program, based on the metric matrix approach (*37*), was utilized to calculate an ensemble of structures fulfilling holonomic (constitutional) and experimental (proton−proton distances) restraints (*38*−*40*). Restrained molecular dynamics was carried out starting with a low-energy DG structure for 600 ps in the H_2O/decane simulation cell at 300 K as described for CCK_A-R(1−47); the force constant for distance restraints was 1000 kJ mol^{-1} nm^{-1}. This was followed by 200 ps of MD in the absence of experimental distance restraints (free MD) to test the energetic stability of the structure.

Intermolecular NOEs from a NOESY spectrum obtained at 308 K with a mixing time of 350 ms were used to determine the structural features of the complex. The final structure of the 600 ps MD calculations of CCK-8 was placed in the two-phase simulation cell (6804 water and 252 decane molecules) approximately 10 Å from the structure of CCK_A-R(1−47) obtained from the MD simulation, to allow the intermolecular NOEs to drive the approach of the ligand to the receptor during the simulated annealing calculations. The elevated temperature used during the simulated annealing was chosen to provide the system with sufficient energy to explore different relative orientations of receptor/ligand compatible with the NOEs. The experimentally derived intramolecular [for both CCK_A-R(1−47) and CCK-8] and intermolecular (between the receptor fragment and the peptide ligand) distance restraints were applied with a force constant of 1000 kJ mol^{-1} nm^{-1}. The previously described simulated annealing protocol was applied, followed by 250 ps of MD at 300 K. Finally, the system was subjected to an additional 250 ps of MD at 300 K without the intermolecular NOEs. One iteration took approximately 0.45 s using five processors of an SGI Origin 2000.

RESULTS

CCK_A-R(1−47). The receptor fragment, CCK_A-R(1−47), consists of the full N-terminal, extracellular domain of CCK_A-R plus a few amino acids of TM1 (Figure 1). Interestingly the solid phase synthesis provided a peptide that spontaneously oxidized, forming a disulfide bridge between the cysteine residues at positions 18 and 29 in the sequence. The oxidation phenomenon was complete and confirmed by mass spectrometry and NMR analysis. No dimerization through intermolecular disulfide bonds was observed. The formation of a disulfide bond between residues

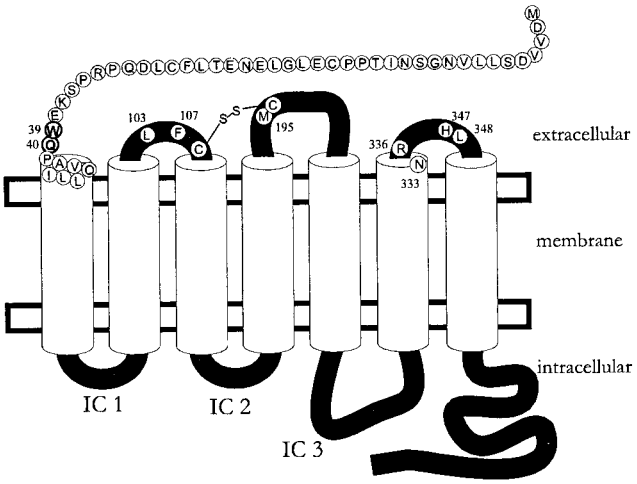

FIGURE 1: Serpentine representation of the CCK_A receptor illustrating the amino acid sequence of CCK_A-R(1−47). Residues shown to contribute to ligand binding in the extracellular loops and discussed in the text are highlighted.

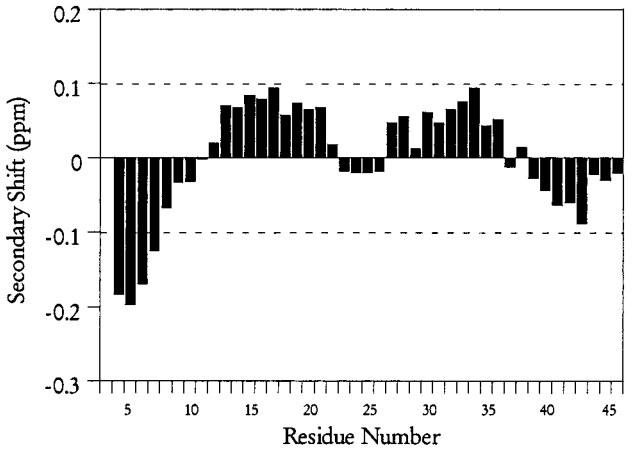

FIGURE 2: The secondary shifts of the Hα protons of CCK_A-R(1−47). The chemical shifts were measured from a TOCSY spectrum (τ_{mix} = 65 ms, T = 35 °C).

distal from each other in the sequence (10 residues apart) is indicative of a preferred folded conformation that places C18 and C29 in close spatial proximity. The oxidized receptor fragment was utilized for the subsequent conformational studies. Reduction of the disulfide bonds in the closely related CCK_B receptor abolishes all affinity for the natural ligand, supporting the conclusion that the disulfide bonds between the extracellular cystines are required for biological function (*7*).

The association of CCK_A-R(1−47) with the micelles is evident by the increase in the line width of the ^1H signals, characteristic of the large molecular weight of the lipid-associated peptide. The high concentration of lipid micelles (171 mM DPC leading to approximately 4 mM micelles) ensures that all of the CCK_A-R is micelle-bound in a nonaggregated state [a micelle:CCK_A-R(1−47) ratio of over 2.5], as testified by the presence of only one set of signals (*41*, *42*).

The secondary shift analysis of CCK_A-R(1−47) in H_2O/DPC is reported in Figure 2. The values are consistent with α-helical structures at the N- and C-termini and two β-strands separated by a turn for the central part of the receptor fragment (*43*). The β-sheet conformation would place C18

Table 1: Nontrival Interresidue NOEs Utilized in the Structure Calculation of CCK_A-R(1−47)[a]

residue 1	atom 1	residue 2	atom 2	distance (Å)	residue 1	atom 1	residue 2	atom 2	distance (Å)
3	HN	4	HN	3.00	4	Hα	7	HN	3.20
4	HN	5	HN	3.00	5	Hα	8	HN	3.20
6	HN	7	HN	3.00	6	Hα	9	HN	3.20
7	HN	8	HN	3.00	37	Hα	40	HN	3.20
8	HN	9	HN	3.00	39	Hα	42	HN	3.20
9	HN	10	HN	3.00	38	HN	42	βCH3	5.00
11	HN	12	HN	3.00	41	Hα	44	CH3 γ1,2	6.00
13	HN	14	HN	3.00	45	HN	42	βCH3	4.00
14	HN	15	HN	3.00	23	Hα	25	HN	3.20
19	HN	20	HN	3.00	39	Hϵ3	40	Hα	3.50
20	HN	21	HN	3.00	39	Hϵ3	41	Hδ1,2	3.50
21	HN	22	HN	4.00	39	Hϵ3	37	Hγ1,2	4.00
22	HN	23	HN	3.00	39	Hϵ3	37	HN	4.00
23	HN	24	HN	3.00	39	Hϵ3	40	HN	4.00
25	HN	26	HN	3.00	39	Hδ1	36	Hα	4.00
26	HN	27	HN	4.00	39	Hδ1	38	Hα	3.50
27	HN	28	HN	3.00	39	Hδ1	38	HN	4.00
29	HN	30	HN	4.00	39	Hδ1	40	HN	4.00
31	HN	32	HN	3.00	39	Hζ2	41	Hα	4.00
38	HN	39	HN	3.00	28	Hϵ1,2	23	Hγ1,2	4.00
39	HN	40	HN	3.00	28	Hϵ1,2	23	Hβ1,2	4.00
42	HN	43	HN	3.00	28	Hϵ1,2	26	CH3	5.00
43	HN	44	HN	3.00	28	Hδ1,2	26	CH3	5.00
45	HN	46	HN	3.00	28	Hδ1,2	26	Hβ	5.00
46	HN	47	HN	3.00	28	Hδ1,2	26	Hα	5.00
7	HN	9	HN	4.20	28	Hδ1,2	23	Hβ1,2	5.00
38	HN	40	HN	4.20	28	Hδ1,2	27	CH3 δ1,2	6.00
10	δNH2	6	Hα	5.00					

[a] The upper bound distance is reported.

and C29 in close proximity, in agreement with the spontaneous formation of a disulfide bridge between these residues. The NOEs, given in Table 1, confirm the presence of the α-helices and β-sheet. Unfortunately, many of the Hα-Hα NOEs (characteristic of a β-sheet conformation) cannot be unambiguously assigned because of spectral crowding. The turn between the strands of the β-sheet is indicated by a distinctive Hα(i)−HN(i+2) NOE between E23 and E25 and by a number of correlations involving the side chains of E23 and F28.

Upon addition of 5-doxylstearic acid to the solution of CCK_A-R(1−47), NMR signals in close proximity to the radical (located at approximately the level of the phosphate headgroup) are significantly broadened (data not shown) (*44*−*46*). Most of the residues show a reduced intensity, indicating that a majority of the amino acids are proximal to the charged membrane surface. In particular, the N-terminal helix displays a periodicity that indicates an α-helix lying on the surface (i.e., the hydrophilic residues projecting into the solution are distal from the nitroxide radical). Similar observations were reported for a fragment of the N-terminus of the parathyroid hormone receptor (*30*). The C-terminal helix is homogeneously affected, as expected for a domain embedded in the micelle in the proximity of the surface. A number of hydrophilic residues in the central portions of the molecule are not affected by the free radical, and presumably project toward the solvent.

Extensive NOE-restrained MD simulations using a H_2O/decane simulation cell were carried out to refine the structural features of CCK_A-R(1−47). The experimentally determined topological orientation was found to be energetically favorable and maintained throughout the simulation [we have previously shown that peptides placed in unfavorable orientations quickly reorient in the two-phase simulation cell (*30*)]. Structures taken from the final 50 ps of the MD simulation are shown superimposed in Figure 3, using the backbone atoms for superposition producing an average RMSD of 1.1 Å (2.1 Å all heavy atoms). No NOE violation greater than 0.2 Å was observed during the simulation. The β-sheet of the central portion of the fragment is indicated by interstrand hydrogen bonds involving both backbone, e.g., $S36_{HN}$−$L8_{CO}$ populated for ca. 85% of the simulation, and side chains, e.g., S12, N13, T15, and D31. The presence of two proline residues in each of the β-strands (P16, P17 and P33, P35), interrupting the hydrogen-bonding pattern, leads to ϕ,ψ values which deviate from the values of a standard β-sheet. The irregularity of the β-sheet is in agreement with the rather small extent of the secondary-shift deviation. The β-sheet is certainly stabilized by a number of hydrophobic amino acids (e.g., I14, L20, L22, L27, and F28) interacting with the membrane.

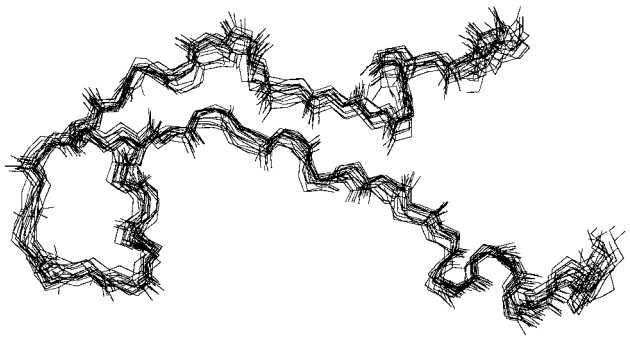

FIGURE 3: Superposition of 17 structures of CCK_A-R(1−47) sampled during the last 50 ps of the NOE-restrained MD simulation in a H_2O/decane cell. Only the backbone atoms and the C18−C29 disulfide bridge are displayed. All backbone atoms were utilized for the superposition. The N-terminus of the receptor fragment is at the top right corner of the figure.

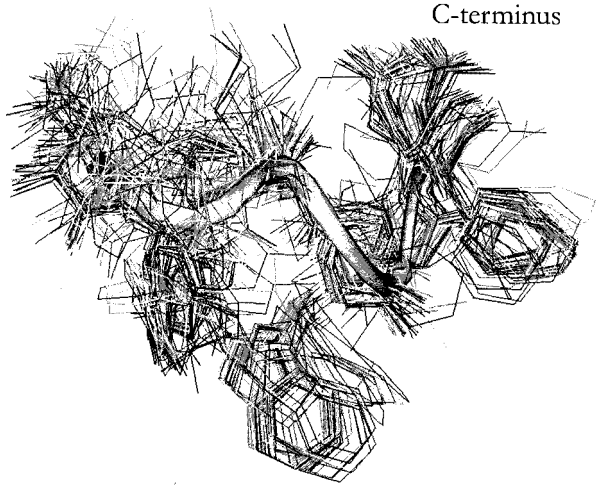

FIGURE 4: Superposition of the 90 structures obtained from the DG calculations of CCK-8 (heavy atoms). Heavy backbone atoms of residues 27−32 are used for the superposition. One of the structures is represented as a ribbon.

Table 2: Values of the ϕ,ψ Dihedral Angles (±standard deviation) for CCK-8 in H_2O/DPC Averaged over the Last 100 ps of the MD Simulations

residue	ϕ	ψ
Tyr^{27}	67 ± 8	-23 ± 18
Met^{28}	-63 ± 16	-7 ± 16
Gly^{29}	-29 ± 15	-45 ± 10
Trp^{30}	-37 ± 8	-42 ± 8
Met^{31}	-114 ± 8	-19 ± 22
Asp^{32}	-104 ± 21	71 ± 11
Phe^{33}	-119 ± 16	79 ± 63

CCK-8. CCK-8 promptly associates with the DPC micelles, as shown by the line broadening and by the sign of the cross-peaks in NOESY spectra. A large number of medium-range NOEs identified from NOESY spectra indicate a well-defined secondary structure, characterized by *i*,*i*+2 and *i*,*i*+3 correlations involving both backbone and side-chain protons (a list of distances is supplied in Supporting Information). The 90 structures resulting from DG calculations, shown superimposed in Figure 4, illustrate a high degree of convergence evidenced by ϕ,ψ dihedral angle order parameters greater than 0.8 (data not shown). During the 600 ps of molecular dynamics, the average RMSD calculated for all backbone atoms is of 0.9 ± 0.1 Å with no significant (over 0.2 Å) NOE violations. The average dihedral angles over the last 100 ps are listed in Table 2. The structure undergoes only minimal changes during the subsequent 200 ps of free MD (removal of the NOE restraints), indicating that the structural features are energetically stable.

CCK$_A$-R(1−47)/CCK-8 Complex. The association of CCK-8 and CCK$_A$-R(1−47) was characterized by titration of the ligand to the receptor fragment monitored by 1D and 2D NMR. One-dimensional ^{1}H spectra collected during the titration are depicted in Figure 5. In the spectral region of interest, the resonances of the aromatic protons of W39 and F28 of the receptor and Tyr^{27}, Trp^{30}, and Phe^{33} of the ligand can be observed. The signals from Tyr^{27}, Phe^{33}, F28, and the 2H proton of Trp^{30} and W39 are well resolved. Unfortunately, the other protons of the two tyrptophan residues resonate at coincident frequencies. Upon addition of CCK-8, the only signal of the receptor to be affected is

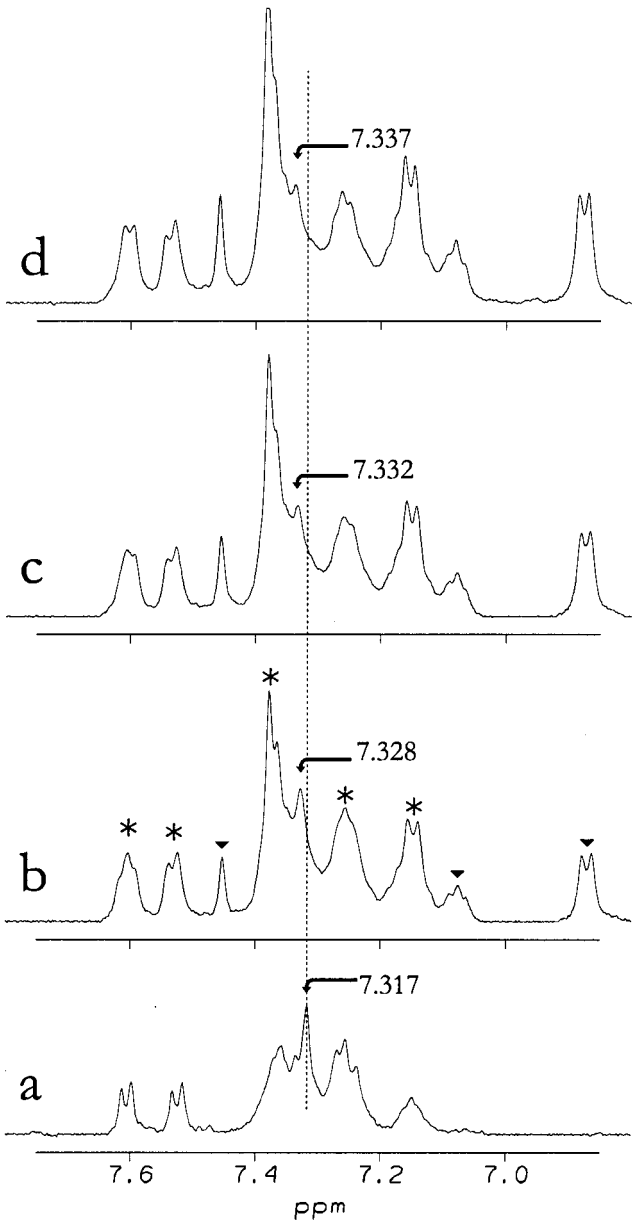

FIGURE 5: Expanded portion of one-dimensional NMR spectra of the receptor fragment, CCK$_A$-R(1−47), upon titration of CCK-8. The spectra were collected at 500 MHz, $T = 298$ K, pH 6.5. The resonance of 2H of W39 is indicated by the frequency in parts per million. (a) CCK$_A$-R(1−47) alone. (b) Addition of 500 μg of CCK-8. The resolved peaks from CCK-8 are labeled with triangles; peaks from CCK-8 overlapping with those of the receptor are denoted with an asterisk. (c) Addition of 750 μg of CCK-8. (d) Addition of 1000 μg of CCK-8.

2H of W39. The signal shifts from 7.317 to 7.337 ppm upon addition of 1 mg of CCK-8. Similar chemical shift perturbations have been recently reported for the binding of C5a anaphylatoxin to the N-terminus of the C5a receptor (*47*). The NOESY spectrum confirms the interaction of CCK-8 with W39 of CCK$_A$-R(1−47) and identifies the residues of the ligand involved in the interaction. Figure 6 shows the NOE cross-peaks involving the 2H proton of W39 and the Hα of Tyr^{27} and Met^{28} of CCK-8. A very weak NOE to the Hα of Asp^{26} is visible in the spectrum at a lower threshold, but due to its low intensity was not utilized in the refinement calculations. The presence of additional intermolecular NOEs originating from W39 (or any other residue of the receptor)

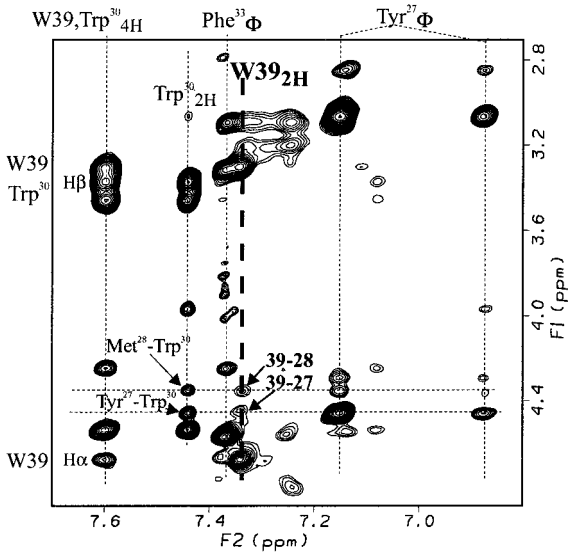

FIGURE 6: Expanded portion of a two-dimensional NOESY spectrum of the CCK-8/CCK_A-R(1−47) complex. The unambiguously assigned intermolecular NOEs between Tyr^{27} and Met^{28} of the ligand and W39 of the receptor fragment are denoted by 39−27 and 39−28, respectively. Some of the intramolecular NOEs indicating a helical conformation of CCK-8, Tyr^{27}-Trp^{30}, and Met^{28}-Trp^{30}, are denoted. See text for experimental details.

cannot be excluded, but they cannot be unambiguously assigned due to resonance overlap [unfortunately, the 47 residues of CCK_A-R(1−47) in DPC micelles are at the limit of resolution of ^{1}H NMR, even at 750 MHz].

A parallel titration of CCK_A-R in DPC micelles with Lys-Kallidin (K-K-R-P-P-G-F-S-P-F-R), under identical conditions as utilized for the titration with CCK-8, proved absolutely no interaction between the N-terminus of CCK_A-R and the unrelated peptide hormone. The ^{1}H spectrum of CCK_A-R was completely unaffected by the addition of up to 1.6 mg of Lys-Kallidin; careful examination of one-dimensional and two-dimensional TOCSY spectra illustrated no deviations in chemical shifts during the titration. Two-dimensional NOESY spectra, collected after the final addition of Lys-Kallidin, displayed no additional NOE peaks. These results clearly exclude nonspecific association of CCK-8 to CCK_A-R(1−47); the intermolecular NOEs observed above are ligand specific. A nonspecific association is not likely given the high affinity of both CCK-8 and CCK_A-R(1−47) for the micelles and the high micelle:peptide ratio utilized during the study of the complex.

The results of the simulated annealing calculations of the CCK-8/CCK_A-R(1−47) complex are depicted in Figure 7. The conformational features of the two separate molecules do not vary during the formation of the complex in the NOE-restrained MD simulation, in agreement with the experimental data. A further 250 ps of MD upon removal of intermolecular NOEs confirmed that the complex is energetically stable in the absence of experimental restraints. The general topology consists of the α-helix of hydrophobic residues at the C-terminus of CCK_A-R(1−47), corresponding to the top of TM1, embedded in the decane layer, with the pseudo-helix of CCK-8 aligned in almost a parallel fashion. The complex is stabilized by a number of hydrophobic and Coulombic interactions. The hydrophobic interactions are provided by the close proximity of the side chains of Tyr^{27} to P35 and W39, Met^{28} to W39 and A42, and Met^{31} to L46.

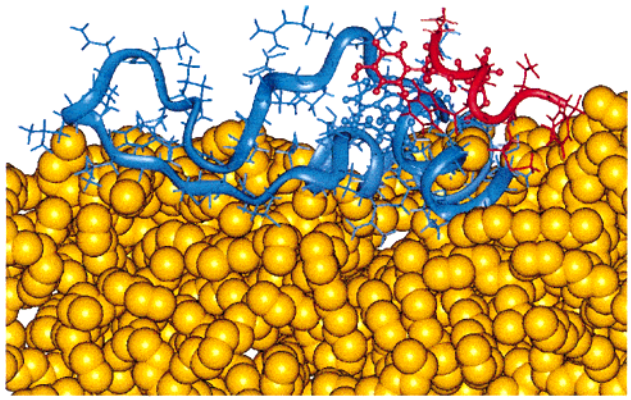

FIGURE 7: The structure of the complex of CCK_A-R(1−47) and CCK-8 as resulting form NOE-restrained simulated annealing calculations followed by 250 ps of NOE-restrained MD simulation and by 250 ps of unrestrained MD. All simulations were carried out in a periodic H_2O/decane cell. The receptor fragment and CCK-8 are shown as ribbons in blue and red, respectively. The decane molecules are depicted as CPK in gold. Residues Tyr^{27}, Met^{28} of CCK-8 and W39, and Q40 of CCK_A-R(1−47) are displayed in ball-and-stick. The C-terminus of the receptor fragment lays on the front of the box, the N-terminal helix points away from the reader, approximately in the middle of the figure. Water is not displayed for clarity.

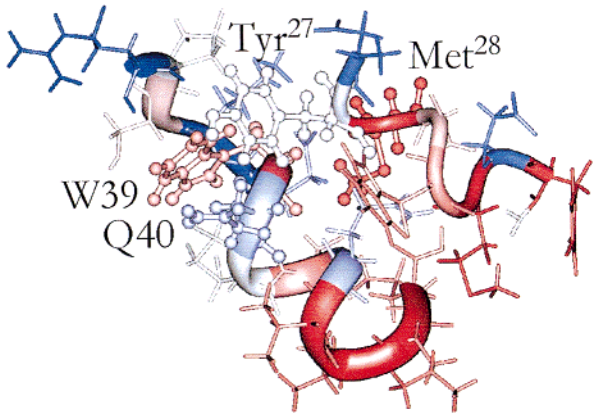

FIGURE 8: Particular of the complex of CCK_A-R(1−47) and CCK-8, displayed in its entirety in Figure 7. The residues Tyr^{27} and Met^{28} of CCK-8 and W39 and Q40 of CCK_A-R(1−47) are displayed in ball-and-stick. The residues are colored according to hydrophobicity (blue = polar, red = hydrophobic); the solvents are not displayed for clarity.

Numerous Coulombic interactions between Asp^{26} of the ligand and K37, E38, and Q40 of CCK_A-R(1−47) also help stabilize the complex. Some of these features are illustrated in Figure 8. Back calculation of NOEs of the ligand/receptor complex, produces a number of proton−proton contacts involving residues P33, P35-Q40, A42, Q43, L46, and L47 of the receptor and Tyr^{27}-Met^{31} of the ligand. The predicted NOEs involve side-chain protons that are in very crowded regions in the experimental NOESY spectra and therefore cannot be unambiguously identified nor differentiated from the numerous intramolecular NOEs present for both the ligand and receptor. The structural calculations of the ligand/receptor complex have used only those NOEs that could be unambiguously assigned as intermolecular.

DISCUSSION

Our approach to investigate the molecular interaction of CCK-8 with CCK_A-R utilizes NMR and computer simula-

tions to determine the structural features of the ligand and the N-terminal fragment of the receptor implicated in binding and then the complex of the two components. A detailed conformational analysis in the appropriate solvent environment can afford the spatial distribution of key residues, their orientation relative to the membrane interface, and their availability for intermolecular interactions. The NMR studies were carried out in an aqueous solution containing DPC micelles, which provide a hydrophobic core and a zwitterionic surface (phosphate and choline groups) that mimic the biological membrane, while allowing high-resolution NMR experiments (*30*, *41*, *42*, *44*, *48*−*58*). The orientation of the receptor fragment relative to the micelle interface was determined by NMR relaxation studies in the presence of a free-radical-bearing fatty acid (5-doxylstearate) (*44*, *52*). These NMR data, utilized in distance geometry calculations and extensive molecular dynamics simulations, yield the high-resolution structures of the N-terminus of the receptor, CCK_A-R(1−47), and CCK-8.

Upon the formation of the ligand/receptor complex, neither CCK-8 nor CCK_A-R(1−47) undergo major conformational changes as witnessed by the lack of variation of the NMR data. Instead, the structure assumed by CCK-8 in the presence of DPC micelles is the one that binds to the N-terminal receptor fragment. This observation is in agreement with the theory of a membrane-bound pathway for the interaction of peptide hormones with their G-protein coupled receptors (*51*, *59*−*62*). This hypothesis states that the ligand first interacts with the membrane, inducing the peptide to adopt a specific conformation, and then through a two-dimensional translation, the peptide hormone interacts with the extracellular portion of the receptor. It is therefore the membrane-associated conformation of the ligand that first interacts and is recognized by the receptor (*62*).

The receptor/ligand interaction was proven to be ligand specific, as titration with a nonrelated peptide showed no effect on the spectra of the receptor fragment. Furthermore, the residues involved in the receptor/ligand contact as determined by NMR are in agreement with the results from the mutational studies of Fourmy and co-workers (*5*). Ligands of eight or more amino acids in length were affected by W39F and Q40N mutations, while smaller ligands, seven residues or less, showed binding affinities similar to those observed for the wild-type receptor (*5*). This suggests that residues N-terminal of Tyr^{27} are in close proximity with W39 and Q40. The structural features obtained here and intermolecular NOEs between Asp^{26}, Tyr^{27}, and Met^{28} and W39 are consistent with this mode of ligand binding.

This depiction of ligand binding is in stark contrast to the conclusions drawn from a study utilizing photoaffinity cross-linking of CCK-8 to CCK_A-R (*10*). On the basis of a cross-linking point between W39 of the receptor and Phe^{33} of the ligand, the authors propose that the C-terminus of the ligand is proximal to TM1 of the receptor. It must be noted that as a part of this study, the ligand was assumed to adopt a β-hairpin-type conformation (*10*), not consistent with the structures determined experimentally here and previously reported elsewhere (*63*). We hypothesize that the introduction of the *p*-nitro functionality results in a binding mode slightly different from that of the natural peptide, creating a shift in the ligand/receptor alignment. Indeed the binding affinity of the modified ligand is 10-fold lower. Importantly, in the pseudo-helical conformation of CCK-8, experimentally established here, Phe^{33} is in close spatial proximity to residues Tyr^{27}−Met^{28} (a distance of 5.4 Å between Phe^{33} Cζ, bearing the p-NO_2 group, and Met^{28} Cα). Indeed, in the NMR investigation of CCK-8, we observed NOEs between the α protons of Gly^{29} and the C-terminal amide and Phe^{33} HN. Therefore, the altered binding mode of the *p*-nitro ligand required to be consistent with the cross-linking data is minor, and the interpretation of the data may need to be revised in light of the results presented here.

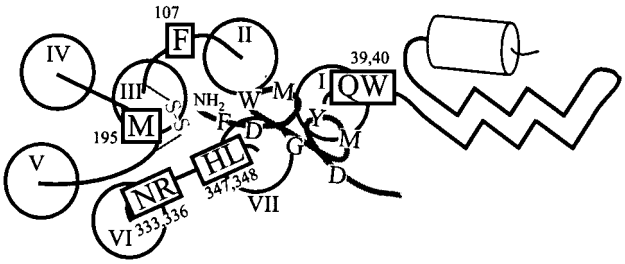

FIGURE 9: Schematic representation of the ligand binding of CCK-8 to CCK_A-R. Many of the residues of CCK_A shown to play a vital role in ligand binding have been included (square boxes) and are elaborated in the text. The close proximity of Tyr^{27} and Met^{28} of CCK-8 to W39 of CCK_A was experimentally verified in this study.

Previous investigations have shown that the extracellular loops play an important role in ligand binding (*7*, *64*). Mutagenesis studies suggest that two hydrophobic amino acids from the first extracellular loop, L103 and F107, are important for ligand binding (particularly F107) (*7*). Recently, H207 of the second extracellular loop and N333/R336 of the third extracellular loop have been shown to interact with the C-terminal residue of CCK-8 (*12*, *13*). A second contact point derived from cross-linking studies has recently appeared, using a ligand with Bpa in place of Gly^{29} (*11*). As expected, this modification is not very well tolerated, leading to a decrease in affinity of over 1000-fold. Despite this drop in binding, a contact point between position 29 of CCK and H347 and L348 in the third extracellular loop could be established (*11*).

These experimental data are consistent with the C-terminus of the ligand in close proximity with the central core of the seven-helical bundle of CCK_A-R. In Figure 9, we depict schematically a binding mode consistent with the experimental data generated here and much of the data in the current literature. In this binding mode, the C-terminal Phe^{33}-NH_2 of CCK-8 would be in close proximity to the extracellular loops and the residues noted above. In addition, the ligand entering the seven helical bundle through TM1 and TM7 would place residue 29 of CCK in close proximity to the third extracellular loop, and the bulky, hydrophobic Bpa would be favorably located near H347 and L348. Therefore, the binding mode depicted in Figure 9 is in accord with the results from cross-linking (*11*). Determination of the structural features of the remaining extracellular portions of the CCK_A receptor, the extracellular loops, will provide the insight required to assign molecular roles of these domains in ligand binding. Efforts along these lines are currently underway in our laboratories.

It is not clear that the data presented here delineating the mode of ligand binding to CCK_A are generally applicable to the closely related CCK_B receptor. The manner in which CCK binds to the CCK_B receptor-subtype is currently an

open question. Mutagenesis data suggesting an alternative mode of binding have appeared (*7*, *65*), while recent photoaffinity cross-linking results are consistent with CCK binding in a fashion similar to both receptor-subtypes (*66*).

In summary, we have determined the structure of CCK-8 and the N-terminal fragment of CCK_A-R consisting of the first 47 amino acids. From unambiguous intermolecular NOEs, the orientation of the ligand relative to the receptor fragment was determined. It is clear that in the native receptor system there could be important receptor/receptor contacts not characterized in this study. However, the close association of CCK_A-R(1−47) with the membrane environment provides a milieu close to the one experienced in the intact receptor, with the lipid playing a determinant role in inducing the correct folding. A similar approach was successfully utilized in the study of the proximal N-terminal fragment of the parathyroid hormone receptor (*30*). Concerning the ligand, although the lipid-induced helical conformation observed here is energetically favorable, interactions between CCK-8 and the native receptor (e.g., extracellular loops) could certainly induce alternative structural features. However, an induced fit of the ligand is not necessarily required for receptor activation. Instead, we hypothesize an initial recognition event between the membrane-associated ligand, helical in conformation, and the N-terminus of CCK_A, also associated with the membrane. The role of this specific interaction is to induce the proper orientation of the C-terminus of the ligand toward the 7 TM helical bundle. The interactions between the C-terminus of the ligand and the receptor (mainly located in the extracellular loops or extracellular ends of the TM helices) produce the translations/rotations of the TM helices thought to be involved in receptor activation (*67*, *68*).

ACKNOWLEDGMENT

We acknowledge the assistance of Chris Turner (MIT) with the use of the 750 MHz instrument (supported through grant RR-00995) and Frank Delaglio (NIH/NIDDK) for use of NMRPipe.

SUPPORTING INFORMATION AVAILABLE

Table of NOE derived distances for CCK-8. This material is available free of charge via the Internet at http://pubs.acs.org.

REFERENCES

1. Silvente-Poirot, S., Dufresne, M., Vaysse, N., and Fourmy, D. (1993) *Eur. J. Biochem. 215*, 513−29.
2. Wank, S. A., Pisegna, J. R., and de Weerth, A. (1992) *Proc. Natl. Acad. Sci. U.S.A. 89*, 8691−5.
3. Wank, S. A., Harkins, R., Jensen, R. T., Shapira, H., de Weerth, A., and Slattery, T. (1992) *Proc. Natl. Acad. Sci. U.S.A. 89*, 3125−9.
4. Wank, S. A. (1995) *Am. J. Physiol. 269*, G628−46.
5. Kennedy, K., Gigoux, V., Escrieut, C., Maigret, B., Martinez, J., Moroder, L., Frehel, D., Gully, D., Vaysse, N., and Fourmy, D. (1997) *J. Biol. Chem. 272*, 2920−6.
6. Gigoux, V., Escrieut, C., Silvente-Poirot, S., Maigret, B., Gouilleux, L., Fehrentz, J. A., Gully, D., Moroder, L., Vaysse, N., and Fourmy, D. (1998) *J. Biol. Chem. 273*, 14380−6.
7. Silvente-Poirot, S., Escrieut, C., and Wank, S. A. (1998) *Mol. Pharmacol. 54*, 364−71.
8. Jagerschmidt, A., Guillaume, N., Roques, B. P., and Noble, F. (1998) *Mol. Pharmacol. 53*, 878−85.
9. Blaker, M., Ren, Y., Gordon, M. C., Hsu, J. E., Beinborn, M., and Kopin, A. S. (1998) *Mol. Pharmacol. 54*, 857−63.
10. Ji, Z., Hadac, E. M., Henne, R. M., Patel, S. A., Lybrand, T. P., and Miller, L. J. (1997) *J. Biol. Chem. 272*, 24393−401.
11. Hadac, E. M., Pinon, D. I., Ji, Z., Holicky, E. L., Henne, R. M., Lybrand, T. P., and Miller, L. J. (1998) *J. Biol. Chem. 273*, 12988−93.
12. Gigoux, V., Escrieut, C., Fehrentz, J. A., Poirot, S., Maigret, B., Moroder, L., Gully, D., Martinez, J., Vaysse, N., and Fourmy, D. (1999) *J. Biol. Chem. 274*, 20457−64.
13. Silvente-Poirot, S., Escrieut, C., Gales, C., Fehrentz, J. A., Escherich, A., Wank, S. A., Martinez, J., Moroder, L., Maigret, B., Bouisson, M., Vaysse, N., and Fourmy, D. (1999) *J. Biol. Chem. 274*, 23191−7.
14. Kopin, A. S., McBride, E. W., Quinn, S. M., Kolakowski, L. F., Jr., and Beinborn, M. (1995) *J. Biol. Chem. 270*, 5019−23.
15. Huang, S. C., Talkad, V. D., Fortune, K. P., Jonnalagadda, S., Severi, C., Delle Fave, G., and Gardner, J. D. (1995) *Proc. Natl. Acad. Sci. U.S.A. 92*, 10312−6.
16. Kauer, J. C., Erickson-Viitanen, S., Wolfe, H. R., Jr., and DeGrado, W. F. (1986) *J. Biol. Chem. 261*, 10695−700.
17. Wilson, C. J., Husain, S. S., Stimson, E. R., Dangott, L. J., Miller, K. W., and Maggio, J. E. (1997) *Biochemistry 36*, 4542−51.
18. Delaglio, F., Grzesiek, S., Vuister, G. W., Zhu, G., Pfeifer, J., and Bax, A. (1995) *J. Biomol. NMR 6*, 277−93.
19. Rance, M., Sørensen, O. W., Bodenhausen, G., Wagner, G., Ernst, R. R., and Wüthrich, K. (1983) *Biochem. Biophys. Res. Commun. 117*, 458−79.
20. Braunschweiler, L., and Ernst, R. R. (1983) *J. Magn. Reson. 53*, 521−8.
21. Bax, A., and Davis, D. G. (1985) *J. Magn. Reson. 65*, 355−60.
22. Jeener, J., Meier, B. H., Bachmann, P., and Ernst, R. R. (1979) *J. Chem. Phys. 71*, 4546−53.
23. Macura, S., Huang, Y., Suter, D., and Ernst, R. R. (1981) *J. Magn. Reson. 43*, 259−81.
24. Piotto, M., Saudek, V., and Sklenar, V. (1992) *J. Biomol. NMR 2*, 661−5.
25. Sklenar, V., Piotto, M., Leppik, R., and Saudek, V. (1993) *J. Magn. Reson., Ser. A 102*, 241−245.
26. Plateau, P., and Gueron, M. (1982) *J. Am. Chem. Soc. 104*, 7310−7311.
27. Wüthrich, K. (1986) *NMR of Proteins and Nucleic acids*, Wiley, New York.
28. Pastore, A., and Saudek, V. (1990) *J. Magn. Reson. 90*, 165−176.
29. van der Spoel, D., van Buuren, A. R., Apol, E., Meulenhoff, P. J., Tieleman, D. p., Sijbers, A. L. T. M., van Drunen, R., and Berendsen, H. J. C. (1996) *Gromacs User Manual*, University of Groningen.
30. Pellegrini, M., Bisello, A., Rosenblatt, M., Chorev, M., and Mierke, D. F. (1998) *Biochemistry 37*, 12737−43.
31. van Buuren, A. R., Marrink, S., and Berendsen, H. J. C. (1993) *J. Phys. Chem. 97*, 9206−16.
32. Berendsen, H. J. C., Postma, J. P. M., DiNola, A., and Haak, J. R. (1984) *J. Chem. Phys. 81*, 3684−90.
33. Hess, B., Bekker, H., Berendsen, H. J. C., and Fraaije, J. G. E. M. (1997) *J. Comput. Chem. 18*, 1463−72.
34. Cavanagh, J., Fairbrother, W. J., Palmer, A. G., and Skelton, N. J. (1996) *Protein NMR Spectroscopy, Principle and Practice*, Academic Press, New York.
35. Wüthrich, K., Billeter, M., and Braun, W. (1983) *J. Mol. Biol. 169*, 949−61.
36. Weber, P. L., Morrison, R., and Hare, D. (1988) *J. Mol. Biol. 204*, 483−7.
37. Havel, T. F. (1991) *Prog. Biophys. Mol. Biol. 56*, 43−78.
38. Mierke, D. F., Geyer, A., and Kessler, H. (1994) *Int. J. Pept. Protein Res. 44*, 325−31.
39. Mierke, D. F., Kurz, M., and Kessler, H. (1994) *J. Am. Chem. Soc. 116*, 1042−9.
40. Pellegrini, M., Gobbo, M., Rocchi, R., Peggion, E., Mammi, S., and Mierke, D. F. (1996) *Biopolymers 40*, 561−9.

41. Kallick, D. A., Tessmer, M. R., Watts, C. R., and Li, C. (1995) *J. Magn. Reson., Ser. B 109*, 60−5.
42. McDonnel, P. A., and Opella, S. J. (1993) *J. Magn. Reson., Ser. B 102*, 120−5.
43. Wishart, D. S., Sykes, B. D., and Richards, F. M. (1992) *Biochemistry 31*, 1647−51.
44. Brown, L. R., Bösch, C., and Wüthrich, K. (1981) *Biochim. Biophys. Acta 642*, 296−312.
45. van de Ven, F. J., van Os, J. W., Aelen, J. M., Wymenga, S. S., Remerowski, M. L., Konings, R. N., and Hilbers, C. W. (1993) *Biochemistry 32*, 8322−8.
46. Pellegrini, M., Royo, M., Chorev, M., and Mierke, D. F. (1996) *J. Pept. Sci. 40*, 653−66.
47. Chen, Z., Zhang, X., Gonnella, N. C., Pellas, T. C., Boyar, W. C., and Ni, F. (1998) *J. Biol. Chem. 273*, 10411−9.
48. Kessler, H., Mierke, D. F., Saulitis, J., Seip, S., Steuernagel, S., Wein, T., and Will, M. (1992) *Biopolymers 32*, 427−33.
49. Strickland, L. A., Bozzato, R. P., and Kronis, K. A. (1993) *Biochemistry 32*, 6050−7.
50. Willis, K. J. (1994) *Int. J. Pept. Protein Res. 43*, 23−8.
51. Moroder, L., Romano, R., Guba, W., Mierke, D. F., Kessler, H., Delporte, C., Winand, J., and Christophe, J. (1993) *Biochemistry 32*, 13551−9.
52. Papavoine, C. H. M., Konings, R. N. H., Hilbers, C. W., and van de Ven, F. J. M. (1994) *Biochemistry 33*, 12990−7.
53. van den Berg, B., Tessari, M., Boelens, R., Dijkman, R., Kaptein, R., de Haas, G. H., and Verheij, H. M. (1995) *J. Biomol. NMR 5*, 110−21.
54. Pellegrini, M., Mammi, S., Peggion, E., and Mierke, D. F. (1997) *J. Med. Chem. 40*, 92−8.
55. Bösch, C., Brown, L. R., and Wüthrich, K. (1980) *Biochem. Biophys. Res. Commun. 95*, 1504−9.
56. Bairaktari, E., Mierke, D. F., Mammi, S., and Peggion, E. (1990) *Biochemistry 29*, 10090−6.
57. Lee, K. H., Fitton, J. E., and Wüthrich, K. (1987) *Biochim. Biophys. Acta 911*, 144−53.
58. Pellegrini, M., Royo, M., Rosenblatt, M., Chorev, M., and Mierke, D. F. (1998) *J. Biol. Chem. 273*, 10420−7.
59. Schwyzer, R. (1995) *Biopolymers 37*, 5−16.
60. Schwyzer, R. (1995) *J. Mol. Recognit. 8*, 3−8.
61. Lutz, J., Romano-Gotsch, R., Escrieut, C., Fourmy, D., Matha, B., Muller, G., Kessler, H., and Moroder, L. (1997) *Biopolymers 41*, 799−817.
62. Moroder, L. (1997) *J. Pept. Sci. 3*, 1−14.
63. Moroder, L. A. D. U., Picone, D., Amodeo, P., and Temussi, P. A. (1993) *Biochem. Biophys. Res. Commun. 190*, 741−6.
64. Wank, S. A. (1998) *Am. J. Physiol. 274*, G607−13.
65. Silvente-Poirot, S., and Wank, S. A. (1996) *J. Biol. Chem. 271*, 14698−706.
66. Anders, J., Bluggel, M., Meyer, H. E., Kuhne, R., ter Laak, A. M., Kojro, E., and Fahrenholz, F. (1999) *Biochemistry 38*, 6043−55.
67. Elling, C. E., Thirstrup, K., Nielsen, S. M., Hjorth, S. A., and Schwartz, T. W. (1997) *Ann. N. Y. Acad. Sci. 814*, 142−51.
68. Bourne, H. R. (1997) *Curr. Opin. Cell Biol. 9*, 134−42.

BI991272L